
A Wrapper to Use a Machine-Learning-Based Algorithm for Earthquake Monitoring

Retailleau Lise ^{1,*}, Saurel Jean-Marie ¹, Zhu Weiqiang ³, Satriano Claudio ¹, Beroza Gregory C. ³, Issartel Simon ⁴, Boissier Patrice ^{1,2}, Ovpf Team ^{1,2}, Ovsm Team ^{1,5}

¹ Université de Paris, Institut de Physique du Globe de Paris, CNRS, Paris, France

² Observatoire Volcanologique du Piton de la Fournaise, Institut de Physique du Globe de Paris, La Plaine des Cafres, La Réunion, France

³ Department of Geophysics, Stanford University, Stanford, California, U.S.A.

⁴ Ecole et Observatoire des Sciences de la Terre, Strasbourg, France

⁵ Observatoire Volcanologique et Sismologique de Martinique, Institut de Physique du Globe de Paris (OVSM-IPGP), Habitation Blondel—Morne la Rosette—Route de l'ancien observatoire, Saint-Pierre, Martinique, France

* Corresponding author : Lise Retailleau, email address : retailleau@ipgp.fr

Abstract :

Seismology is one of the main sciences used to monitor volcanic activity worldwide. Fast, efficient, and accurate seismicity detectors are crucial to assess the activity level of a volcano in near-real time and to issue timely warnings. Traditional real-time seismic processing software uses phase onset pickers followed by a phase association algorithm to declare an event and estimate its location. The pickers typically do not identify whether the detected phase is a P or S arrival, which can have a negative impact on hypocentral location quality and complicates phase association. We implemented the deep-neural-network-based method PhaseNet to identify in real time P and S seismic waves on data from one- and three-component seismometers. We tuned the Earthworm binder_ew associator module to use the phase identification from PhaseNet to detect and locate the events, which we archive in a SeisComP3 database. We assessed the performance of the algorithm by comparing the results with existing catalogs built to monitor seismic and volcanic activity in Mayotte and the Lesser Antilles region. Our algorithm, which we refer to as PhaseWorm, showed promising results in both contexts and clearly outperformed the previous automatic method implemented in Mayotte. This innovative real-time processing system is now operational for seismicity monitoring in Mayotte and Martinique.

1 Introduction

Active volcanoes are among the most impressive signs of deep earth processes threatening populations as in the case of Montagne Pelée in 1902 (Fisher & Heiken, 1982). Volcanic unrest can evolve quickly into a dangerous eruption, with dramatic impacts (e.g. Ontake in 2014 (Kato et al., 2015) and Stromboli in 2019 (Giudicepietro et al., 2020)). Volcanic activity is accompanied by different types of seismic signals that manifest the complex processes occurring within volcanoes (McNutt, 1996), including rock fracture or the movement of magmatic and volatile components (Chouet, 1996). A strong relationship thus exists between seismicity changes and eruption onset (e.g., in Piton de la Fournaise, (Peltier et al., 2009)) or changes in eruptive style (Saint-Vincent Soufrière in 2021 (National Emergency Management Organisation of St. Vincent and the Grenadines Website, 2021)). For this reason, volcano observatories need comprehensive and real-time monitoring of their recorded seismicity. Rapid reaction is crucial in the case of volcanic unrest to alert civil security authorities (Peltier et al., 2021).

46 Automatic seismicity detection and location is usually divided in two main steps:
47 a phase arrival detection on each data stream followed by a phase association to iden-
48 tify events from coherent incoming arrivals across a seismic network. Classical real-time
49 detection methods rely on the observation of energy variation through a characteristic
50 function like STA/LTA (Allen, 1978) or kurtosis (Baillard et al., 2014). These methods
51 have been proven useful on many occasions, in many settings, and have the great advan-
52 tage of requiring little computational power. A drawback, however, is that they do not
53 identify the picked phase type (P or S-wave), which has to be determined by further pro-
54 cessing during phase association. Moreover, the balance between detection of small event
55 and reliable picking can prove difficult for noisy data, where both false and missed picks
56 may be common.

57 Another approach is template matching (Shelly et al., 2007), where previously iden-
58 tified earthquakes are used to search for events by cross-correlation of known waveforms
59 in continuous data. This method typically detects very small events that would have oth-
60 erwise been missed. It is, however, computationally intensive, requires prior knowledge
61 of template waveforms such that it won't detect new events, which is particularly prob-
62 lematic for real-time monitoring. For these reasons, this method is preferable for pos-
63 terior analysis (Duputel et al., 2019).

64 Methods of similarity search through auto-correlation implies correlating all sig-
65 nals to find events. This methods leads to a thorough search, however, it can be com-
66 putationally demanding and memory intensive, despite efforts to accelerate this process
67 through the use of fingerprints (Yoon et al., 2015). As with template matching, this ap-
68 proach will not detect new events until they repeat, which is disadvantageous for real-
69 time monitoring.

70 New opportunities for rapid event detection have emerged through the application
71 of machine learning methods to seismic monitoring. PhaseNet is a neural-network-based
72 method that can detect P and S waves and estimate their arrival times (Zhu & Beroza,
73 2019). This advantage is extremely helpful for automatic detection and location and we
74 choose PhaseNet for phase detection. Other similar machine-learning algorithms exist
75 (Perol et al., 2018; Mousavi et al., 2020).

76 The association of phases with events is the other crucial step for seismicity anal-
77 ysis. The simplest algorithms look for temporal coherency between the different detected
78 phase arrivals to determine the occurrence of a seismic event. Other methods back-propagate

79 the incoming detected arrivals in time and space, assuming P phases, and declare an event
80 when a cluster of phases reach the configured threshold. Finally, some associators use
81 a grid search algorithm (Weber et al., 2007, SeisComP3,) to find hypothetical hypocen-
82 ters that match the detected phase arrivals. Those algorithms then associate further ar-
83 rivals and bind them to P or S phases to refine the location.

84 Two open software suites are commonly used for operational real-time earthquake
85 analysis: Earthworm (Johnson et al., 1995) and SeisComP3 (Weber et al., 2007). Their
86 performances and capabilities are similar for real-time earthquake detection and loca-
87 tion (Olivieri & Clinton, 2012). Identifying whether a pick is a P- or S-phase without
88 the waveform is complicated, consequently, some associators choose not to deal with S-
89 phases (e.g. SeisComP3). Location is then only constrained by P-phases which can lead
90 to location errors. We choose Earthworm to process PhaseNet picks mainly because it
91 can add S-phases to the event arrivals stack and use them in the location process. This
92 exploits the ability of PhaseNet to detect and distinguish both P and S waves. We use
93 SeisComP3 to calculate the event magnitudes and store the locations in a database be-
94 cause it provides modern graphical user interfaces that analysts can use to manually val-
95 idate and revise each event location. Indeed, picks are checked daily at the Institut de
96 physique du globe de Paris (IPGP) observatories where PhaseWorm was installed.

97 We build a Python wrapper to use the method PhaseNet for seismic phase detec-
98 tion and send the results to the processing package Earthworm for event association and
99 location. We then use the processing package SeisComP3 for magnitude calculation, cat-
100 aloguing, and manual event review. We first present the different steps of the process,
101 then present its application and real-time implementation for monitoring tectonic and
102 volcanic seismic activity in Mayotte and Martinique. We call our wrapper PhaseWorm
103 for practicality in a way to shorten its designation.

104 **2 Process**

105 Figure 1 summarizes the different steps of the process we developed.

106 **2.1 Data request and pre-processing**

107 We download and pre-process the data using the package ObsPy (Krischer et al.,
108 2015). PhaseWorm can be configured to acquire data from a Seedlink, a WaveServerV

109 or an FDSN dataselect server or from a disk archive. We download 30 s segments of 3-
110 components data for each station, which we demean and taper before resampling at 100
111 Hz, whatever the input sample-rate (Figure 1). When working on 1-component stations,
112 we duplicate the Z channel to create 2 horizontal channels. We overlap the time windows
113 by 50% to avoid missing arrivals at segment borders.

114 Closely located stations (distance less than the associator cell size) can lead to mis-
115 identification of events as both stations detect the same phases. In this case, to avoid
116 these spurious detections, we assign both stations the same alias so that they are con-
117 sidered as a single multi-sensor station, although their SCNL (Station, Channel, Net-
118 work, Location code) may be different.

119 **2.2 Phase detection with PhaseNet**

120 PhaseNet is a deep-neural-network-based method trained to identify P and S wave
121 arrivals (Zhu & Beroza, 2019). It was trained using data from the Northern California
122 Earthquake Catalog to recognize the main body wave arrivals from 3 component seis-
123 mograms, from broadband, short-period, or accelerometer sensors, and was engineered
124 so that the classification probability would peak at the labelled arrival time.

125 Although trained on data from Northern California, PhaseNet has generalized well
126 to measure arrival times from Southern California in the Ridgecrest earthquake sequence
127 (Liu et al., 2020), from induced seismicity in the Central US (Park et al., 2020), and to
128 the Appenines in Italy (Tan et al., 2021). For that reason, and because it was effective
129 in tests we carried out at Mayotte (“Automatic detection of the seismicity associated to
130 the Mayotte volcanic crisis”, 2020, Retailleau et al., in review), we did not retrain the
131 model with local data.

132 PhaseNet identifies P and S arrivals (Figure 1) on each 30 s of pre-processed 3-channels
133 waveform data. We convert and write PhaseNet picks as TYPE_PICK_SCNL Earthworm
134 messages. 50% data overlap can lead to duplicate picks that are filtered by Earthworm
135 if they share a common network/station stream and a pick time difference smaller than
136 0.05s. P-picks are mapped to the vertical channels and S-picks to the horizontal chan-
137 nels. PhaseNet calculates a probability for each pick, which we convert to Earthworm
138 pick weights (from 3 to 0, from low to high quality).

139 **2.3 Event identification with Earthworm**

140 Earthworm is a modular real-time seismic processing software package that has been
141 developed since the early 1990s (Johnson et al., 1995). The heart of the automatic lo-
142 cation process is the binder_ew module based on the Auryn phase associator (Johnson
143 et al., 1995). The associator back-propagates new picks in a 4D time and space matrix,
144 assuming they are P-phases and using a 1D velocity model. When a given number of picks
145 gather into the same cells, an earthquake is declared and an arrivals stack initiated (Fig-
146 ure 1). Further picks can then be associated either as S or P phases. We configure the
147 module binder_ew to stack P-phases only from vertical channels and S-phases only from
148 horizontal channels. This ensures that PhaseNet phase identifications are optimally re-
149 ported and used.

150 Once the arrivals stack has reached a minimum level of various quality indicators,
151 it is forwarded to the location modules, which depend on each observatory (NonLinLoc
152 (Lomax, 2008) in Mayotte and Hypo71 (Lee & Lahr, 1975) in Martinique).

153 **2.4 Cataloguing with SeisComP3**

154 SeisComP3 (Weber et al., 2007) is a seismic processing software package that pro-
155 vides data acquisition and real-time processing modules, an event database with multi-
156 origin capabilities, and numerous graphical user interfaces (GUI).

157 When located by Earthworm, the resulting HYPO2000_ARC message is sent to Seis-
158 ComP3. The message is parsed and the serialized picks, arrivals and origin objects are
159 sent to the SeisComP3 messaging system. SeisComP3 creates a new event, or updates
160 an existing one, with this new origin, while dedicated modules compute magnitudes, cho-
161 sen according each observatory’s practice. SeisComP3 scmag (Gempa, 2020) can com-
162 pute a dozen different magnitudes.

163 We can also feed SeisComP3 automatic locations from other sources using the same
164 software or exposing their location on an FDSN webservice. While the PhaseWorm so-
165 lution is always preferred, this allows us to store all the origins in the same database and
166 to perform comparisons between our PhaseWorm implementation and existing automatic
167 and manual locations and detections (Figure 1).

3 Analysis of the Mayotte seismicity

Mayotte island is located in the Comoros archipelago (Figure 2a) and is part of a wider volcanic zone (e.g., Famin et al., 2020). Before 2018, the most recent volcanic activity was dated to 4000 years ago on Mayotte (Zinke et al., 2003). A phase of strong seismicity initiated in May 2018 (Cesca et al., 2020; Lemoine et al., 2020) associated with a new major submarine eruption that led to the formation of a new volcanic edifice (NVE) discovered in May 2019 (Feuillet et al., 2021, red triangle in Figure 2a,).

The seismicity is mainly located in two clusters (Feuillet et al., 2021). One cluster (distal cluster) is parallel to the N120 submarine volcanic ridge leading to the NVE 2a, and the other (proximal cluster) is closer, 5 to 15km from Petite-Terre island 2a, where fluid emissions from the sea-floor have been observed and mapped during marine surveys since 2019 (Feuillet, N. and Jorry, S. and Rinnert, E. and Thinon, I. and Fouquet, Y., 2019).

3.1 Monitoring seismicity in real time

Numerous earthquakes have been felt, particularly at the beginning of the crisis in 2018 (27 with associated PGA above $0.1m.s^{-2}$). Earthquakes continue to be regularly felt, so the crisis is ongoing and a reactivation of volcanic areas closer to or on Mayotte is a possibility. Consequently, comprehensive real-time monitoring of the active areas through their seismicity is crucial.

We implement and test our wrapper and Earthworm configuration to identify in near real time the ongoing seismicity recorded by Mayotte land stations. While only one seismic station was installed on the island before the beginning of the seismic crisis in 2018, efforts have been made to deploy more stations to monitor the seismic activity (Figure 2a and Saurel et al. (2019)). Stations on the islands were mostly installed in early 2019 in reaction to the crisis and are located in places affected by anthropogenic noise.

From early 2019 to February 2021, the automatic detection of the seismicity in Mayotte was carried out by BCSF/ReNaSS (Bureau central de sismologie Français, Réseau National de surveillance sismique) using SeisComP3 software. Arrivals were detected using an STA/LTA algorithm and events identified using a grid search algorithm and the IASPEI91 velocity model. Because there are only 8 stations in Mayotte, detections were declared with a minimum of 4 coherent arrivals. Locations were finally obtained using

199 LocSAT and IASPEI91 model, using only the P-waves. Because STA/LTA is affected
200 by noisy stations, the threshold was increased to avoid false detections, resulting in lim-
201 ited sensitivity to low magnitude earthquakes.

202 **3.2 Implementation at the Observatory**

203 The Observatoire volcanologique du Piton de la Fournaise (OVPF) is in charge of
204 the daily monitoring of Mayotte volcanic activity since February 2020 to discern any change
205 in behavior. Until March 2021, the automatic detection of the seismicity was the same
206 as the one that had been used by BCSF/ReNaSS, using STA/LTA for arrival detection.

207 To guarantee robustness and reliability, OVPF operates a virtualization cluster with
208 3 redundant pro-grade servers, network, and storage. In case of hardware failure for one
209 of the 3 servers, the embedded software ensures an automatic and even distribution of
210 the virtual machines on the 2 remaining servers.

211 This cluster hosts a virtual machine (VM) dedicated to PhaseNet and Earthworm
212 instances. The Earthworm associator uses 2.5 km cells and locations are made with Non-
213 LinLoc (Lomax, 2008) using a setup developed during Mayobs1 (Saurel et al., 2019) with
214 the local velocity model from ?. The Earthworm results are sent to the existing SeisComP3
215 VM dedicated to Mayotte. We show a comparison example of the phase picks obtained
216 with the manual method and the previous and new automatic methods in Figure 2b. All
217 three methods detect the P arrivals. The manual (red) and new method (with PhaseNet
218 in blue) match very well while the picks from the method used previously tend to be late
219 (SeisComP3 in green). Moreover, the SeisComP3 process we used did not detect S waves.
220 The manual and PhaseNet S wave picks (red and blue respectively) fit quite well.

221 We impose a delay of 30 s before starting each data segment process to ensure that
222 all the waveforms have reached the data server. The data retrieval, pre-processing and
223 phase detection using PhaseNet take about 2 s. We configured Earthworm phase asso-
224 ciator to update the preliminary event location every 5 s to integrate new arrivals. We
225 then wait 20 s for the associator to have added all the coherent phase picks with a sta-
226 ble preliminary location. We follow by doing the final location with NonLinLoc. Finally,
227 the magnitude M_l calculation and the event cataloging by SeisComP3 takes less than
228 2 s.

3.3 A two-month test

Using the retrospective mode, we compared our new process to the method that was previously used at the observatory over two months of data (December 2020 and January 2021).

We first compare the identification statistics between the two automatic methods and the manual identification (performed through visualization of continuous 1-component timeseries). We analyse the statistics for the two main types of seismicity observed by Mayotte land stations: Volcano-Tectonic (VT) events with energy between 1 and 40Hz and Long Period (LP) events with energy between 0.5 and 5Hz.

Figure 3a represents the daily histograms of the VT events previously identified by SeisComP3 (light green), the manual identification (medium green), and the new automatic method we call PhaseWorm (dark green). These results show that the new method is very successful in identifying the VT seismicity compared to the manual identification, and particularly compared to SeisComP3.

On the other hand, only 15% of the manually identified LP are detected by the new process (Figure 3b). Missed LP events are not caused by a lack of phase detection by PhaseNet, but rather by the fact that the Earthworm associator can only declare an event using P waves, which are usually very weak for LP events. Making binder_ew aware of P and S readings and able to use S-phases during the stack initialization would certainly increase both the number of detected events and the robustness of the detection. A collaboration with Instrumental Software Technologies, Inc. (ISTI) is planned to add this capabilities. We conjecture that adding the S-phases to declare events will lead to an identification of LP earthquakes as efficient as manual identifications since their S-phases are detected correctly with PhaseNet. Still, the PhaseWorm method does identify many more LP events than does SeisComP3, which identified only three LP events during the test period. Training PhaseNet on manual picks of the Mayotte seismicity could help improve PhaseNet's capability to pick S phases of LP earthquakes. Unfortunately, P arrivals are usually also difficult to pick manually. This implies that there may not be enough labels to permit a useful training of PhaseNet for this purpose.

In Figure 3c we represent, for the two-month test period, the automatic locations obtained with SeisComP3 and the newly implemented (PhaseWorm) methods. The pre-

260 viously used method was not able to locate events correctly because it missed too many
261 arrivals, did not use S-phases and used a global velocity model. The new PhaseWorm
262 method location results correctly highlight the two main clusters of seismicity.

263 Following these successful results, the algorithm has been operational since March
264 1st, 2021 at OVPF for the daily monitoring of the seismic activity in Mayotte. It ran in
265 parallel with the old method for approximately ten days. Results were similar to our two-
266 month test: with many more detections and locations compared with the previous method.
267 After these ten days, the previous method was turned off.

268 4 Implementation at Martinique Observatory

269 4.1 Seismicity in the Lesser Antilles

270 A variety of types of earthquakes are recorded in subduction zones: volcanic ac-
271 tivity related earthquakes, crustal earthquakes in the upper plate, intermediate-depth
272 earthquakes in the slab, and interface earthquakes on the subduction front.

273 In the Caribbean, the Lesser Antilles is a relatively slow convergence rate subduc-
274 tion zone where the North American plate and the Caribbean plate converge at between
275 2 and 3.4 cm per year (Bernard & Lambert, 1988). Despite this slow rate, there were
276 two major devastating thrust earthquakes in the nineteenth century (Bernard & Lam-
277 bert, 1988): in 1839, a M 8.0 event destroyed Fort Royal (now Fort de France) in Mar-
278 tinique and in 1843, a M 8.5 event destroyed Pointe à Pitre in Guadeloupe.

279 Brown et al. (2015) showed that the Lesser Antilles territories and countries are
280 some of the most vulnerable ones to volcanic hazards in the world. In Martinique, Mon-
281 tagne Pelée volcano is known for its deadly 1902 eruption that killed 29,000 people in
282 the cities of Saint-Pierre and Morne Rouge. More recently, in April 2021, only 2 weeks
283 after a seismicity pattern change (National Emergency Management Organisation of St.
284 Vincent and the Grenadines Website, 2021), an explosive eruption occurred at La Soufrière
285 on Saint-Vincent Island, producing major tephra fallout and pyroclastic flows. Thanks
286 to an accurate real-time seismic monitoring, 20,000 inhabitants of endangered areas were
287 evacuated, and no casualties were reported (Seismic Research Center, 2021).

288 Active volcanoes of the Lesser Antilles and regional seismicity are monitored by
289 networks of seismic stations operated by IPGP in Martinique (triangles on Figure 4) and

290 Guadeloupe, and by the Seismic Research Center of the University of the West Indies
291 (SRC-UWI) in most of the English-speaking islands. Other networks also operates sta-
292 tions on some of the Lesser Antilles islands. Over the last 20 years, there is evidence that
293 the inter-plate seismicity has significantly increased offshore Martinique (Corbeau et al.,
294 2021) together with an increase of locally felt events. Starting in late 2019, the Montagne
295 Pelée seismicity slowly rose and a swarm of VT events occurred in October 2020 together
296 with minutes-long low frequency tremors (OVSM-IPGP, 2020). These changes imply a
297 pressing need for a robust automatic event detection and location algorithm to track any
298 evolution of Montagne Pelée seismicity. The activity is monitored daily by the Obser-
299 vatoire volcanologique et sismologique de Martinique (OVSM). We compare our anal-
300 ysis with their catalog.

301 **4.2 Multi-scale implementation**

302 The co-existence in the same area of a wide range of earthquake sources is a chal-
303 lenge for efficient accurate automatic detection and location. An automated system must
304 be able to deal both with M 0 or less volcanic events within a few hundred of meters of
305 the stations and with powerful subduction events that occur hundreds of kilometers away.
306 Moreover, the station distribution is strongly variable with dense monitoring around the
307 volcanoes and much more diffuse regional monitoring across the islands aligned with the
308 subduction. A single PhaseWorm instance produces arrivals for all the stations, which
309 feed 3 associator modules and pipelines with different configurations to acomodate for
310 the uneven repartition of the stations and work at different scales:

- 311 1. subduction-wide associator using a 5km spaced, 500km side grid and a few sta-
312 tions per island
- 313 2. Martinique associator using a 2km spaced, 200km side grid and stations on the
314 island
- 315 3. Montagne Pelée associator using a dense 0.5km spaced, 25km side grid and sta-
316 tions limited to the volcano

317 All three location pipelines use the same Hypo71PC locator (Lee & Lahr, 1975) follow-
318 ing the configurations already implemented at the observatory. The subduction and Mar-
319 tinique associators use a 1D regional velocity model while the volcano associator uses
320 a specific velocity model for Montagne Pelée volcano.

4.3 VT and tectonic seismicity analysis in Martinique

We analysed one month of data recorded between April 10th and May 10th when both Montagne Pelée VTs and tectonic earthquakes were recorded by Martinique observatory networks. Most of the tectonic earthquakes identified by Martinique observatory were also picked and located with PhaseWorm (Figure 5b). Missing events are usually weak or regional events a few hundreds of km away from the stations. Figure 5c shows that depths are quite accurate despite being spread along the subducting slab. The higher slab angle drawn by the seismicity (compared to the Slab2 model) is consistent with the conclusions of Bie et al. (2020) who used a high-precision earthquake catalog relocated with a temporary OBS network. On Montagne Pelée, the VT activity is mostly composed of repeating earthquakes from a few families (Hirn et al., 1987). In addition to the continuous waveform manual screening, the observatory performs template matching detection. This very sensitive method can retrieve very small events that would have been missed by the operators who manually examine continuous data record daily. These small events can be identified, but are too small to be located. We do not expect PhaseWorm to identify them since they are likely only detected on the few closest stations. For this reason we distinguish between the events in the catalog that are located (dark blue in Figure 5) and those that are not (light blue in Figure 5). PhaseWorm detects and locates most of the VT events that could be manually located by the observatory as shown by Figure 5a. Despite the small number of stations covering the volcano, automatic locations from PhaseWorm also match the pattern from manual locations Figure 4.

5 Conclusions

We developed a wrapper to use the neural network-based PhaseNet picker from several data server types, together with Earthworm (specially tuned) and SeisComP3, which provides a new real-time process to automatically detect and locate earthquakes. We link a phase picking algorithm to event association and location algorithms. Our purpose was to perform high quality seismicity analysis in real-time to enhance the reaction time of observatories monitoring active volcanic systems and their associated tectonic settings. Precise real-time monitoring of seismicity provides essential information for crisis management. With the use of identified P and S waves, our automatic locations are precise enough to be used in preliminary analysis and reports. In the cases of both the Mayotte seismicity and the Montagne Pelée volcano in Martinique, we obtain very satisfactory

353 results - much better than previously used real time methods and close to manual anal-
354 ysis, both in terms of number of detected events and in their location accuracy. We use
355 SeisComP3 for cataloguing and magnitude calculation because we also use it at both ob-
356 servatories for daily manual analysis of the events. We plan to add a python module to
357 calculate the magnitude and build the catalog when no manual analysis a posteriori is
358 needed. Future plans also includes the upgrade of Earthworm associator to use the S phases
359 in the earthquake declaration stage (which should dramatically increase PhaseWorm de-
360 tection capabilities for LP and weak events) and the release of a fully integrated Earth-
361 worm module. PhaseWorm can help monitoring seismicity in real time and reduce the
362 work of analysts. The algorithm has proven very useful to monitor the activity in May-
363 otte since its implementation in March 2021, and is now installed in Martinique, in con-
364 texts very different than where PhaseNet was initially trained.

365 **Data and Ressources**

366 RA network data available from Résif datacenter (<http://seismology.resif.fr> Résif,
367 1995; doi:10.15778/RESIF.RA). ED.MCHI station data available at EduSismo. 1T (Feuil-
368 let, Van der Woerd and RESIF, 2022; doi:10.15778/resif.1t2018) data available upon re-
369 quest at Résif datacenter. AM network data are available from IRIS and Raspberry Shake
370 SA datacenters (Raspberry Shake Community et al, 2016; doi:10.7914/SN/AM). Mar-
371 tinique networks (IPGP, 2021; doi:10.18715/MARTINIQUE.OVSM) data available from
372 IPGP datacenter (<http://volobsis.ipgp.fr>).

373 Figure 2 map was created with QGis. Map bathymetry from Mayobs1 (doi:10.17600/18001217).
374 Data available upon request at SISMER.

375 PhaseWorm source code is available at <https://github.com/jmsaurel/phaseworm>.

376 **Declaration of Competing**

377 The authors declare no competing interests.

378 **Acknowledgments**

379 REVOSIMA (Réseau de surveillance volcanologique et sismologique de Mayotte) funded
380 some of the additional seismic stations in the Mayotte area. Greg Beroza and Weiqiang

381 Zhu were supported by the Department of Energy (Basic Energy Sciences; Award DE-
382 SC0020445).

383 OVPF Team: Aline Peltier, Patrice Boissier, Valérie Ferrazzini, Christophe Brunet,
384 Frédéric Lauret, Nicolas Desfete, Kevin Canjamalé, Cyprien Griot, Lise Retailleau, Philippe
385 Catherine, Philippe Kowalski, Andrea di Muro, Fabrice Fontaine, Luciano Garavaglia.

386 OVSM Team: Jordane Corbeau, Fabrice R. Fontaine, Jean-Gilles Gabriel, Frédéric
387 Jadélus, Jean-Marc Lavenair, David Mélézan, Cyril Vidal, Benoît Zimmermann, Guih-
388 lem Barruol, Marie-Paule Bouin, Arnaud Burtin, Jean-Christophe Komorowski, Angèle
389 Laurent, Arnaud Lemarchand.

390 References

- 391 Allen, R. V. (1978). Automatic earthquake recognition and timing from single
392 traces. *Bulletin of the seismological society of America*, 68(5), 1521–1532.
- 393 Automatic detection of the seismicity associated to the mayotte volcanic crisis.
394 (2020). In *Agu fall meeting abstracts* (Vol. 2020, pp. V040–0002).
- 395 Baillard, C., Crawford, W. C., Ballu, V., Hibert, C., & Mangeney, A. (2014). An
396 automatic kurtosis-based p-and s-phase picker designed for local seismic networks.
397 *Bulletin of the Seismological Society of America*, 104(1), 394–409.
- 398 Bernard, P., & Lambert, J. (1988, 12). Subduction and seismic hazard in the north-
399 ern Lesser Antilles: Revision of the historical seismicity. *Bulletin of the Seismolog-
400 ical Society of America*, 78(6), 1965-1983. Retrieved from [https://doi.org/10](https://doi.org/10.1785/BSSA0780061965)
401 [.1785/BSSA0780061965](https://doi.org/10.1785/BSSA0780061965) doi: 10.1785/BSSA0780061965
- 402 Bie, L., Rietbrock, A., Hicks, S., Allen, R., Blundy, J., Clouard, V., ... Wilson,
403 M. (2020, January). Along arc heterogeneity in local seismicity across the lesser
404 antilles subduction zone from a dense ocean-bottom seismometer network. *Seis-
405 mological research letters.*, 9(1), 237–247.
- 406 Brown, S. K., Loughlin, S. C., Sparks, R., Vye-Brown, C., Barclay, J., Calder,
407 E., ... et al. (2015). Global volcanic hazard and risk. In S. C. Lough-
408 lin, S. Sparks, S. K. Brown, S. F. Jenkins, & C. Vye-Brown (Eds.), *Global
409 volcanic hazards and risk* (p. 81–172). Cambridge University Press. doi:
410 10.1017/CBO9781316276273.004
- 411 Cesca, S., Letort, J., Razafindrakoto, H. N., Heimann, S., Rivalta, E., Isken, M. P.,
412 ... others (2020). Drainage of a deep magma reservoir near mayotte inferred from

- 413 seismicity and deformation. *Nature geoscience*, 13(1), 87–93.
- 414 Chouet, B. A. (1996). Long-period volcano seismicity: its source and use in eruption
415 forecasting. *Nature*, 380(6572), 309–316.
- 416 Corbeau, J., Gonzalez, O., Feuillet, N., Lejeune, A., Fontaine, F., Clouard, V., ...
417 Team, O. (2021). A significant increase in interplate seismicity near major histor-
418 ical earthquakes offshore martinique (fwi). *Bulletin of the Seismological Society of*
419 *America*, 111, 1106–.
- 420 Duputel, Z., Lengliné, O., & Ferrazzini, V. (2019). Constraining spatiotemporal
421 characteristics of magma migration at piton de la fournaise volcano from pre-
422 eruptive seismicity. *Geophysical research letters*, 46(1), 119–127.
- 423 Famin, V., Michon, L., & Bourhane, A. (2020). The comoros archipelago: a right-
424 lateral transform boundary between the somalia and lwandle plates. *Tectono-*
425 *physics*, 789, 228539.
- 426 Feuillet, N., Jorry, S., Crawford, W., Deplus, C., Thinon, I., Jacques, E., ... others
427 (2021). Birth of a large volcanic edifice through lithosphere-scale dyking offshore
428 Mayotte (Indian Ocean). *Nature Geoscience*, in press.
- 429 Feuillet, N. and Jorry, S. and Rinnert, E. and Thinon, I. and Fouquet, Y. (2019).
430 *Mayobs*. Set of cruises.
- 431 Fisher, R. V., & Heiken, G. (1982). Mt. pelée, martinique: May 8 and 20, 1902, py-
432 roclastic flows and surges. *Journal of Volcanology and Geothermal Research*, 13(3-
433 4), 339–371.
- 434 Gempa. (2020). *Seiscomp3 scmag documentation*. [https://docs.gempa.de/
435 seiscomp3/current/apps/scmag.html](https://docs.gempa.de/seiscomp3/current/apps/scmag.html).
- 436 Giudicepietro, F., López, C., Macedonio, G., Alparone, S., Bianco, F., Calvari, S.,
437 ... others (2020). Geophysical precursors of the july-august 2019 paroxysmal
438 eruptive phase and their implications for stromboli volcano (italy) monitoring.
439 *Scientific reports*, 10(1), 1–16.
- 440 Hirn, A., Girardin, N., Viodé, J.-P., & Eschenbrenner, S. (1987, Dec). *Shallow*
441 *seismicity at montagne pelée volcano, martinique, lesser antilles* (Vol. 49) (No. 6).
442 Springer Science and Business Media LLC. Retrieved from [http://dx.doi.org/
443 10.1007/BF01079823](http://dx.doi.org/10.1007/BF01079823) doi: 10.1007/bf01079823
- 444 Johnson, C. E., Bittenbinder, A., Bogaert, B., Dietz, L., & Kohler, W. (1995).
445 Earthworm: A flexible approach to seismic network processing. *Iris newsletter*,

446 14(2), 1–4.

447 Kato, A., Terakawa, T., Yamanaka, Y., Maeda, Y., Horikawa, S., Matsuihiro, K., &
 448 Okuda, T. (2015). Preparatory and precursory processes leading up to the 2014
 449 phreatic eruption of mount ontake, japan. *Earth, Planets and Space*, 67(1), 1–11.

450 Krischer, L., Megies, T., Barsch, R., Beyreuther, M., Lecocq, T., Caudron, C., &
 451 Wassermann, J. (2015). Obspy: A bridge for seismology into the scientific python
 452 ecosystem. *Computational Science & Discovery*, 8(1), 014003.

453 Lee, W., & Lahr, J. (1975). Hypo71pc (1975). a computer program for determin-
 454 ing hypocenter, magnitude and first motion pattern of local earthquakes. *US Geol.*
 455 *surv., open-file report*, 75, 311.

456 Lemoine, A., Briole, P., Bertil, D., Roullé, A., Foumelis, M., Thinon, I., ...
 457 Hoste Colomer, R. (2020). The 2018–2019 seismo-volcanic crisis east of mayotte,
 458 comoros islands: seismicity and ground deformation markers of an exceptional
 459 submarine eruption. *Geophysical Journal International*, 223(1), 22–44.

460 Liu, M., Zhang, M., Zhu, W., Ellsworth, W. L., & Li, H. (2020). Rapid characteri-
 461 zation of the july 2019 ridgecrest, california, earthquake sequence from raw seismic
 462 data using machine-learning phase picker. *Geophysical Research Letters*, 47(4),
 463 e2019GL086189.

464 Lomax, A. (2008). The nonlinloc software guide. *ALomax Scientific, Mouans-*
 465 *Sartoux, France*, <http://alomax.free.fr/nlloc>.

466 McNutt, S. R. (1996). Seismic monitoring and eruption forecasting of volcanoes: a
 467 review of the state-of-the-art and case histories. *Monitoring and mitigation of vol-*
 468 *cano hazards*, 99–146.

469 Mousavi, M., Ellsworth, W., Zhu, W., Chuang, L., & Beroza, G. (2020). Earth-
 470 quake transformer—an attentive deep-learning model for simultaneous earth-
 471 quake detection and phase picking. *Nature Communications*, 11, 3952. doi:
 472 10.1038/s41467-020-17591-w

473 National Emergency Management Organisation of St. Vincent and the
 474 Grenadines Website. (2021). *Scientists have noted a change in seismic*
 475 *activity associated with the ongoing eruption of the la soufrière volcano.*
 476 [http://nemo.gov.vc/nemo/index.php/news-events/news-release/628-scientists-](http://nemo.gov.vc/nemo/index.php/news-events/news-release/628-scientists-have-noted-a-change-in-seismic-activity-associated-with-the-ongoing-eruption-of-the-la-soufriere-volcano)
 477 [have-noted-a-change-in-seismic-activity-associated-with-the-ongoing-eruption-of-](http://nemo.gov.vc/nemo/index.php/news-events/news-release/628-scientists-have-noted-a-change-in-seismic-activity-associated-with-the-ongoing-eruption-of-the-la-soufriere-volcano)
 478 [the-la-soufriere-volcano.](http://nemo.gov.vc/nemo/index.php/news-events/news-release/628-scientists-have-noted-a-change-in-seismic-activity-associated-with-the-ongoing-eruption-of-the-la-soufriere-volcano)

- 479 Olivieri, M., & Clinton, J. (2012). An almost fair comparison between earthworm
480 and seiscomp3. *Seismological Research Letters*, 83(4), 720–727.
- 481 OVSM-IPGP. (2020). *Monthly bulletin on the volcanic activity of la montagne*
482 *pelée and the regional seismicity of martinique*. [http://volcano.ipgp.jussieu](http://volcano.ipgp.jussieu.fr/martinique/Bulletins/2020/OVSM_2020-11_eng.pdf)
483 [.fr/martinique/Bulletins/2020/OVSM_2020-11_eng.pdf](http://volcano.ipgp.jussieu.fr/martinique/Bulletins/2020/OVSM_2020-11_eng.pdf).
- 484 Park, Y., Mousavi, S. M., Zhu, W., Ellsworth, W. L., & Beroza, G. C. (2020).
485 Machine-learning-based analysis of the guy-greenbrier, arkansas earthquakes: A
486 tale of two sequences. *Geophysical Research Letters*, 47(6), e2020GL087032.
- 487 Peltier, A., Bachèlery, P., & Staudacher, T. (2009). Magma transport and storage at
488 piton de la fournaise (la réunion) between 1972 and 2007: A review of geophysical
489 and geochemical data. *Journal of Volcanology and Geothermal Research*, 184(1-2),
490 93–108.
- 491 Peltier, A., Ferrazzini, V., Di Muro, A., Kowalski, P., Villeneuve, N., Richter, N., ...
492 others (2021). Volcano crisis management at piton de la fournaise (la réunion)
493 during the covid-19 lockdown. *Seismological Society of America*, 92(1), 38–52.
- 494 Perol, T., Gharbi, M., & Denolle, M. (2018). Convolutional neural network for
495 earthquake detection and location. *Science Advances*, 4(2), e1700578. doi: 10
496 .1126/sciadv.1700578
- 497 Saurel, J.-M., Aiken, C., Jacques, E., Lemoine, A., Crawford, W. C., Lemarchand,
498 A., ... others (2019). High-resolution onboard manual locations of mayotte
499 seismicity since march 2019, using local land and seafloor stations. In *Agu fall*
500 *meeting abstracts* (Vol. 2019, pp. V43I-0220).
- 501 Seismic Research Center, U. o. t. W. I. (2021). *La soufriere, svg eruption 2020/2021*.
502 <http://uwiseismic.com/General.aspx?id=93>.
- 503 Shelly, D. R., Beroza, G. C., & Ide, S. (2007). Non-volcanic tremor and low-
504 frequency earthquake swarms. *Nature*, 446(7133), 305–307.
- 505 Tan, Y. J., Waldhauser, F., Ellsworth, W. L., Zhang, M., Zhu, W., Michele, M., ...
506 Segou, M. (2021). Machine-learning-based high-resolution earthquake catalog
507 reveals how complex fault structures were activated during the 2016–2017 central
508 italy sequence. *The Seismic Record*, 1(1), 11–19.
- 509 Weber, B., Becker, J., Hanka, W., Heinloo, A., Hoffmann, M., Kraft, T., ... Thoms,
510 H. (2007). Seiscomp3 - automatic and interactive real time data processing.
511 *Geophysical Research Abstracts*, 9(09219).

- 512 Yoon, C. E., O'Reilly, O., Bergen, K. J., & Beroza, G. C. (2015). Earthquake detec-
513 tion through computationally efficient similarity search. *Science advances*, *1*(11),
514 e1501057.
- 515 Zhu, W., & Beroza, G. C. (2019). Phasenet: a deep-neural-network-based seismic
516 arrival-time picking method. *Geophysical Journal International*, *216*(1), 261–273.
- 517 Zinke, J., Reijmer, J., & Thomassin, B. (2003). Systems tracts sedimentology in the
518 lagoon of mayotte associated with the holocene transgression. *Sedimentary Geol-*
519 *ogy*, *160*(1-3), 57–79.

520 **Mailing addresses**

521 Retailleau Lise : Observatoire volcanologique du Piton de la Fournaise, Institut de
522 Physique du Globe de Paris, 14 RN3 - Km 27, F-97418 La Plaine des Cafres, La Réunion,
523 France

524 Saurel Jean-Marie : Université de Paris, Institut de Physique du Globe de Paris,
525 CNRS, 1 rue Jussieu, F-75005 Paris, France

526 Zhu Weiqiang : Department of Geophysics, Stanford University, 397 Panama Mall,
527 Stanford, California, United States of America

528 Satriano Claudio : Université de Paris, Institut de Physique du Globe de Paris, CNRS,
529 1 rue Jussieu, F-75005 Paris, France

530 Beroza Gregory C. : Department of Geophysics, Stanford University, 397 Panama
531 Mall, Stanford, California, United States of America

532 Issartel Simon : Ecole et Observatoire des Sciences de la Terre, 5 rue René Descartes,
533 Strasbourg, France

534 Boissier Patrice : Observatoire volcanologique du Piton de la Fournaise, Institut
535 de Physique du Globe de Paris, 14 RN3 - Km 27, F-97418 La Plaine des Cafres, La Réunion,
536 France

537 OVPF Team : Observatoire volcanologique du Piton de la Fournaise, Institut de
538 Physique du Globe de Paris, 14 RN3 - Km 27, F-97418 La Plaine des Cafres, La Réunion,
539 France

540 OVSM Team : Observatoire Volcanologique et Sismologique de Martinique, Insti-
541 tut de Physique du Globe de Paris (OVSM-IPGP), Habitation Blondel - Morne la Rosette
542 - Route de l'ancien observatoire, Saint-Pierre, Martinique, France

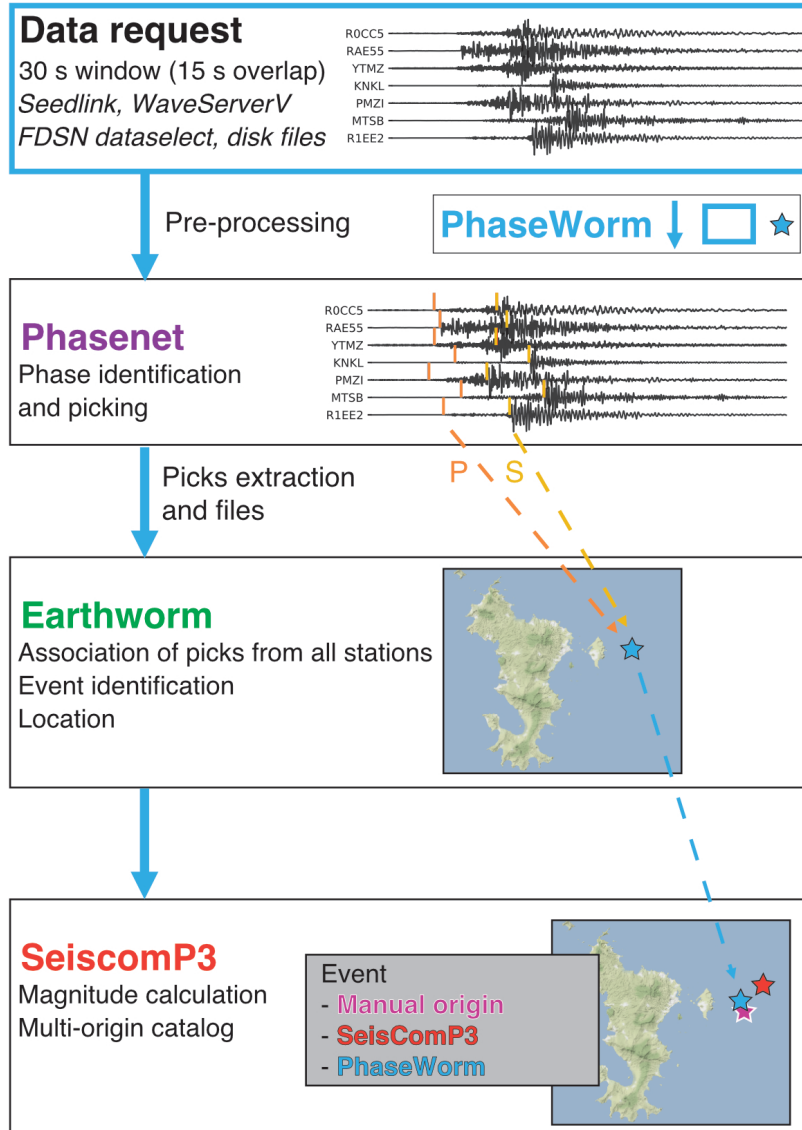


Figure 1. Process developed for the automatic detection and location of seismic events. Blue items represent the PhaseWorm wrapper addition built to to combine the different steps. A more detailed algorithmic flow chart can be found on the PhaseWorm github repository.

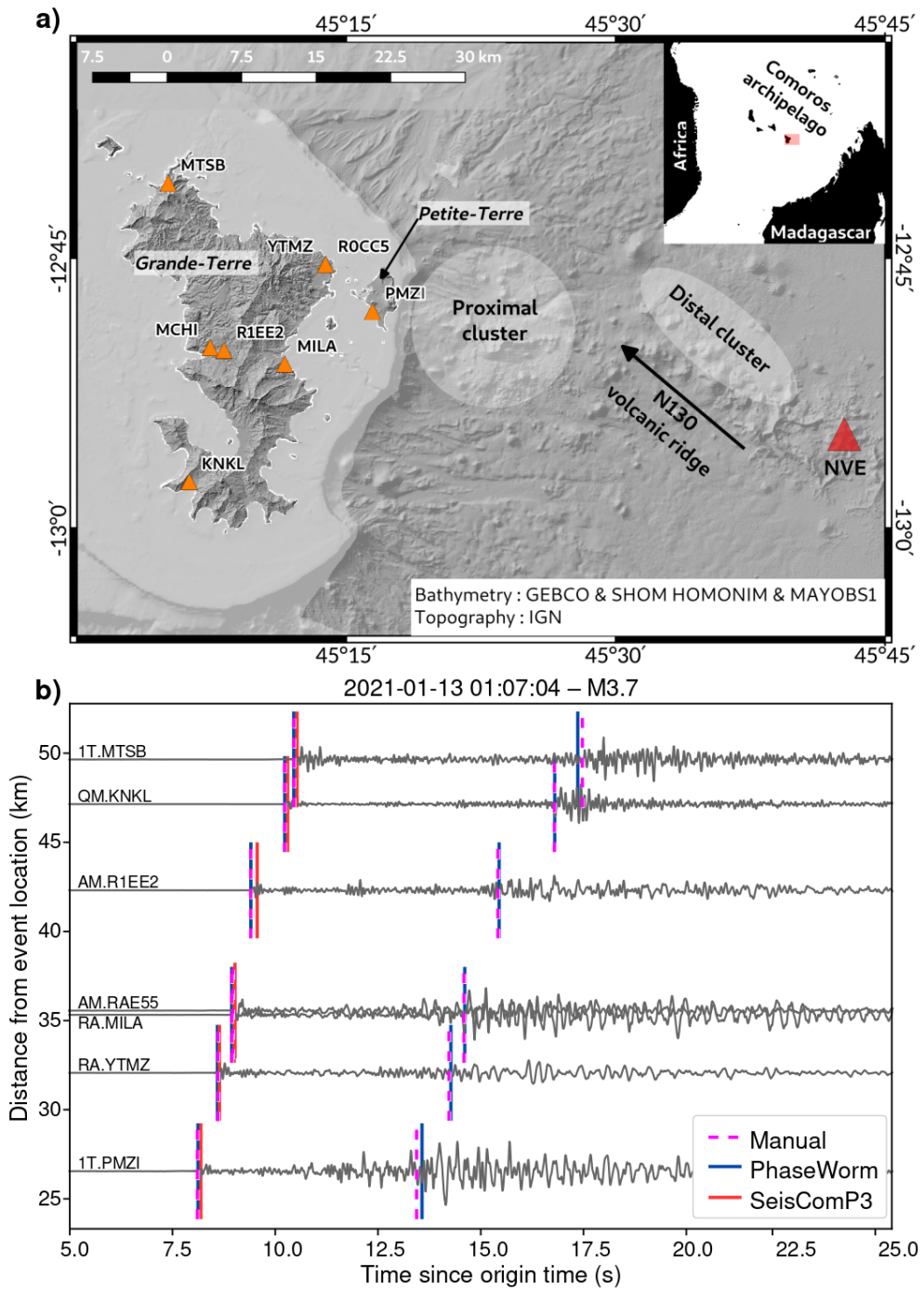


Figure 2. a) Map of the seismic stations in Mayotte (orange triangle), location of the New volcanic edifice (red triangle) and main geographic features. Insert: regional map of the Comoros archipelago, North of Mozambique channel, between Africa and Madagascar. b) Example of picks on a M3.7 event made manually (magenta dashed line), and by PhaseNet (solid blue) and previous SeisComP3 method (solid red). Stations are sorted by distance from the manual location.

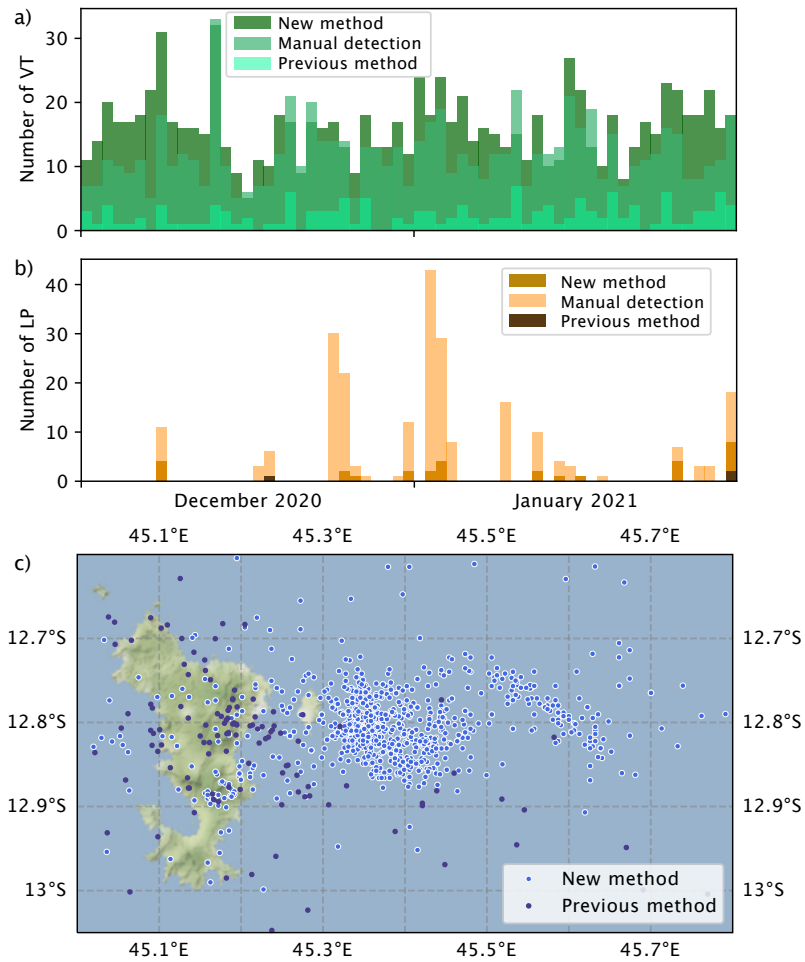


Figure 3. Comparison of the seismicity a,b) detected and c) located by the different methods between December 2020 and January 2021. Daily histograms obtained with SeisComP3, PhaseWorm and the manual identifications for the a) VT and b) LP events.

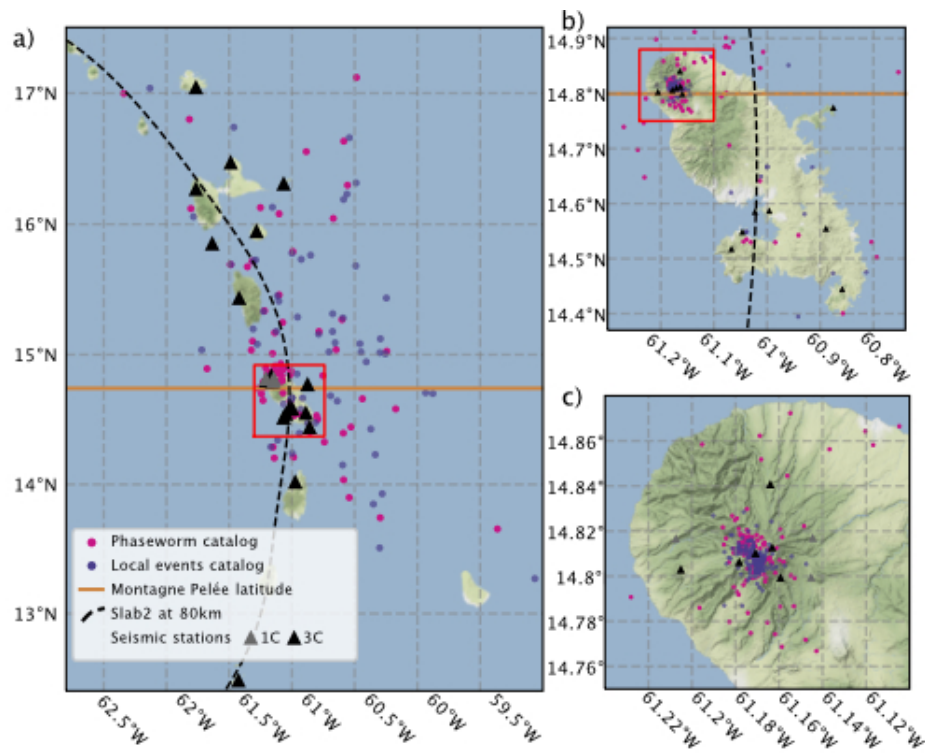


Figure 4. a) Map of the central part of the Lesser Antilles with the IPGP seismic stations used in our study (triangles) and the earthquakes located during our test (dots). Zooms on b) Martinique Island and c) Montagne Pelée.

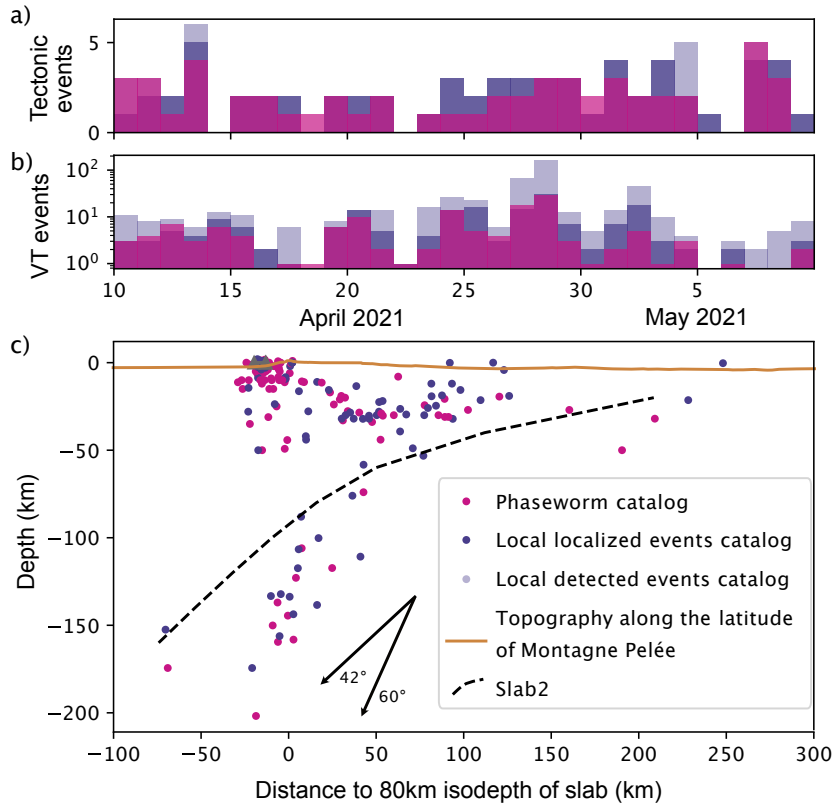


Figure 5. Daily detections during the month of analysis performed for the a) Tectonic and b) Volcano-tectonic events. c) All tectonic and VT events projected on profiles perpendicular to the 80km iso-depth slab contour and represented at the latitude of Montagne Pelée (Figure 4). The dashed line represents the subduction slope from Slab2.